ORIGINAL ARTICLE

A PID-Controlled Approach in the Design of a Physiotherapy Robot for Upper Arm Rehabilitation

Lau Ngee Bing[1] and Ismail Mohd Khairuddin[1]

[1]Faculty of Manufacturing and Mechatronic Engineering Technology, Universiti Malaysia Pahang Al-Sultan Abdullah, 26600 Pahang, Malaysia.

ABSTRACT – The main objective to develop controller for the rebab robot, therefore to achieve the main objective, the subsequent objective is to formulate the mathematical modelling of 2 DOF of upper arm, to develop upper arm rebab robot, evaluate the performance of the controller and facilitate the creation of new and more improved devices for physiotherapy robot ; therefore, this research will investigate rehabilitation robots, it have shown a high potential for improving the patient's mobility, improving their functional movements and assisting in daily activities. However, this technology is still an emerging field and suffers from several challenges like compliance control and dynamic uncertain caused by the human–robot collaboration. The main challenge addressed in this thesis is to develop a controller to the rehab robot and formulate the mathematical modelling of 2 DOF of upper arm. Ensure that the exoskeleton robot provides a suitable compliance control that allows it to cooperate perfectly with humans even if the dynamic model of the exoskeleton robot is uncertain. The PID controller is a widely used control algorithm that aims to regulate a system's output by continuously adjusting its input. In the context of a two-degree-of-freedom (2-DOF) robot arm, the PID controller plays a crucial role in achieving precise and accurate arm movements. The Proportional-Integral-Derivative (PID) controller employs three main components to achieve control: proportional, integral, and derivative terms.

INTRODUCTION

Each year, over 13.7 million people suffer from a stroke and its aftereffects; the elderly are particularly vulnerable. Two-thirds of stroke victims experience some degree of motor impairment [1]. Multiple additional conditions and traumas, such as Guillain-Barré syndrome and stroke, also result in abnormal neuromotor function. However, many people can recover a portion of their lost motor abilities. Thus, neurotherapy can effectively initiate the underlying healing process if administered with sufficient intensity, such as an adequate number of repetitions and a high level of mental and physical participation on the part of the patient.

Rehabilitation robots, a recent advancement in the fields of physiotherapy and assisted mobility, have piqued the interest of many scientists. Robotic upper limb rehabilitation therapy is gaining popularity in the rehabilitation industry as technology advances [2]. It is intended to support or expedite the recovery process by assisting with manual therapy, which is frequently administered by therapists and requires a great deal of repetition [3]. Research on robots is in its infancy due to their complex mechanical construction, the variety of assist techniques they can employ with patients with varying degrees of impairment, and their sensitivity to various human conditions.

Therefore, therapy robots may enable clinicians to devote more time to cognitively demanding aspects of therapy, such as arranging therapy and observing client interactions. As the therapist concentrates more on planning and analysing the course of treatment, and as robot capabilities such as high-intensity training and quantitative analysis are added, it is anticipated that therapy quality will improve [4].

The main objective to develop controller for the rebab robot, therefore to achieve the main objective, the subsequent objective is to formulate the mathematical modelling of 2 DOF of upper arm, to develop upper arm rebab robot, evaluate the performance of the controller and facilitate the creation of new and more improved devices for physiotherapy robot.

The 2-DOF robot arm consists of two interconnected joints that allow for both rotational and translational movements. The PID controller's objective is to control these joints to reach a desired position or trajectory while minimizing any errors or deviations.

The Proportional-Integral-Derivative (PID) controller employs three main components to achieve control, proportional, integral, and derivative terms [5]. The proportional term produces an output based on the current error

between the desired and actual positions of the robot arm. The integral term accounts for accumulated errors over time, enhancing the controller's ability to eliminate steady-state errors. Lastly, the derivative term predicts and responds to the rate of change of the error, enabling the controller to react quickly to sudden disturbances.

By tuning the PID controller's gains, a balance between stability and responsiveness can be achieved, allowing the robot arm to move smoothly and accurately. The controller continuously adjusts the input signals to the robot arm's actuators, ensuring precise control of each joint and enabling the arm to track desired trajectories or perform specific tasks effectively.

RELATED WORK

Analysis control system based on mathematical modelling, open loop analysis, closed loop analysis until last stage of control method application in picture or diagram form, explanation, and flow chart. The best control method is then selected to fulfil the objective of this research. Last but not least, the proper planning is necessary to ensure that the desired result can be achieved.

Phase 1	Phase 2	Phase 3	Phase 4
• Model Plant or system • Derivation of the kinematic equation	• Simulation in MATLAB • Develop PID Controller	• Desgin and develop the rehab robot arm	• Tuning PID • Evaluate the performance of the controller
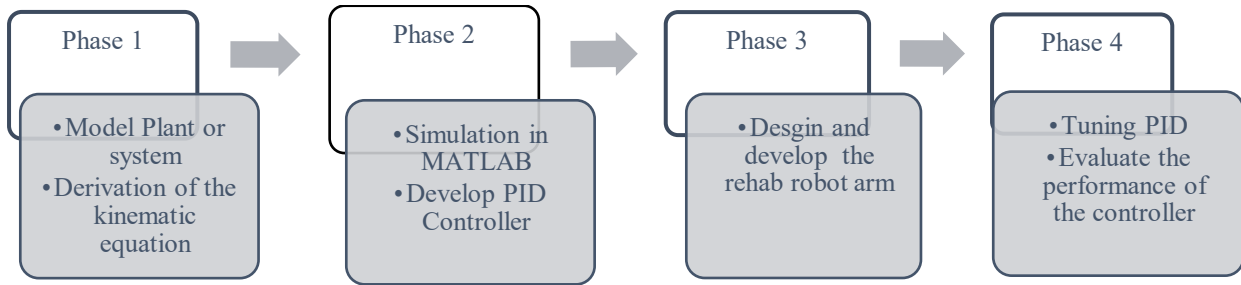
Figure 1. Flow chart

MATHEMATICAL MODELLING
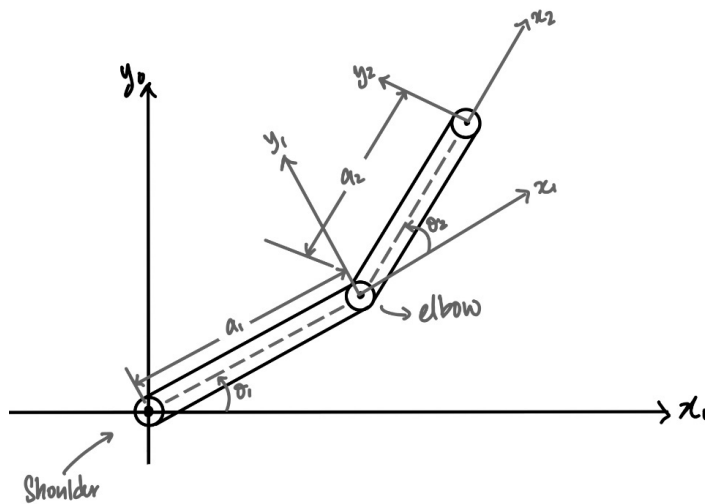
Figure 2. Free Body Diagram in Sagittal Plane

Forward Kinematic

The Denavit-Hartenberg (DH) parameters, a set of variables used to derive homogenous transformation matrices across the various frames assigned to the robot arm structure, are what govern the forward kinematics of the robotic arm[6]. The following definitions describe the DH parameters for a robotic arm with two degrees of freedom:

Table 1. Forward kinematics

Link	a_i	α_i	d_i	θ_i
1	L_1	0	0	θ_1
2	L_2	0	0	θ_2

The following is how the homogenous transformation matrices for the 2-DOF robotic arm in Figure 1 are derived:

$$
{}^0_1T = \begin{bmatrix} \cos\theta_1 & -\sin\theta_1 & 0 & L_1\cos\theta_1 \\ \sin\theta_1 & \cos\theta_1 & 0 & L_1\sin\theta_1 \\ 0 & 0 & 1 & 0 \\ 0 & 0 & 0 & 1 \end{bmatrix} \tag{1}
$$

$$\begin{array}{c} {}^{1}_{2}T \end{array} = \begin{bmatrix} \cos\theta_2 & -\sin\theta_2 & 0 & L_2\cos\theta_2 \\ \sin\theta_2 & \cos\theta_2 & 0 & L_2\sin\theta_2 \\ 0 & 0 & 1 & 0 \\ 0 & 0 & 0 & 1 \end{bmatrix} \tag{2}$$

The position coordinates of the manipulator end-effector is given by:

$$P_X = L_1\cos\theta_1 + L_2\cos(\theta_1 + \theta_2) \tag{3}$$

$$P_y = L_1\sin\theta_1 + L_2\sin(\theta_1 + \theta_2) \tag{4}$$

Inverse Kinematic

The joint variables of an artificial arm are computed using inverse kinematics based on the position of the end-effector in Cartesian space. The mathematical equations of the inverse kinematics problem can be determined algebraically or geometrically. For robot arms with numerous degrees of freedom, it is believed that the geometric approach is significantly simpler [7]. Using geometric solutions, the inverse kinematics equations for Figure 2's two-degree-of-freedom robotic limb were solved.
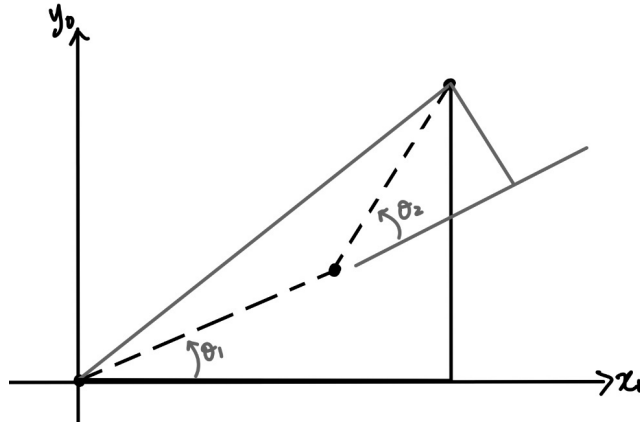
Figure 3. Two degree of freedom Robot Arm Inverse Kinematic

$$P_X{}^2 + P_y{}^2 = L_1{}^2 + L_2{}^2 + 2\,L_1L_2\cos\theta_2 \tag{5}$$

$$\cos\theta_2 = \frac{1}{2\,L_1L_2}\,(P_X{}^2 + P_y{}^2 - L_1{}^2 - L_2{}^2) \tag{6}$$

$$\sin\theta_2 = \pm\ \sqrt{1 - \cos\theta_2{}^2} \tag{7}$$

Therefore,

$$\theta_2 = \pm\,\mathrm{atan}\,\frac{\sin\theta_2}{\cos\theta_2} \tag{8}$$

For the joint variable θ_1:

$$P_X = (L_1 + L_2\cos\theta_2)\cos\theta_2 - L_2\sin\theta_1\sin\theta_2 \tag{9}$$

$$P_y = L_2\sin\theta_2\cos\theta_1 + (L_1 + L_2\cos\theta_2)\sin\theta_1 \tag{10}$$

$$P_X{}^2 + P_y{}^2 = (L_1 + L_2\cos\theta_2)^2 + (L_2\sin\theta_2)^2 \tag{11}$$

$$\Delta\sin\theta_1 = \begin{bmatrix} L_1 + L_2\cos\theta_2 & P_X \\ L_2\sin\theta_2 & P_y \end{bmatrix} \tag{12}$$

$$\Delta\cos\theta_1 = \begin{bmatrix} P_X & -L_2\sin\theta_2 \\ P_y & L_1 + L_2\cos\theta_2 \end{bmatrix} \tag{13}$$

$$\sin \theta_1 = \frac{\Delta \sin \theta_1}{\Delta} = \frac{(L_1 + L_2 \cos \theta_2)P_y - (L_2 \sin \theta_2)P_X}{P_X^2 + P_y^2} \tag{14}$$

$$\cos \theta_1 = \frac{\Delta \cos \theta_1}{\Delta} = \frac{(L_1 + L_2 \cos \theta_2)P_x + (L_2 \sin \theta_2)P_y}{P_X^2 + P_y^2} \tag{15}$$

Robot Dynamic

Force or torque imparted to each joint was calculated using the Eular-Lagrange approach [8], which also served to estimate the Lagrangian (L) of the overall system. This method is based on computing the total kinetic and potential energy of the robot arm [9]. The partial derivative of the kinetic and potential energy attributes of mechanical systems determines the equations of motion in the Euler-Lagrange equation, which is represented as follows.

$$\mathcal{L}(q(t), q(\dot{t})) = K_E(q(t), q(\dot{t})) - P_E(q(t)) \tag{16}$$

$$\begin{bmatrix} x_1 \\ y_1 \end{bmatrix} = \begin{bmatrix} L_1 \cos \theta_1 \\ L_1 \sin \theta_1 \end{bmatrix} \tag{17}$$

$$\begin{bmatrix} \dot{x}_1 \\ \dot{y}_1 \end{bmatrix} = \begin{bmatrix} -L_1 \sin \theta_1 \\ L_1 \cos \theta_1 \end{bmatrix} \dot{\theta}_1 \tag{18}$$

$$\begin{bmatrix} x_2 \\ y_2 \end{bmatrix} = \begin{bmatrix} L_1 \cos \theta_1 + L_2 \cos(\theta_1 + \theta_2) \\ L_1 \sin \theta_1 + L_2 \sin(\theta_1 + \theta_2) \end{bmatrix} \tag{19}$$

$$\begin{bmatrix} \dot{x}_2 \\ \dot{y}_2 \end{bmatrix} = \begin{bmatrix} -L_1 \sin \theta_1 - L_2 \sin(\theta_1 + \theta_2) & -L_2 \sin(\theta_1 + \theta_2) \\ L_1 \cos \theta_1 + L_2 \cos(\theta_1 + \theta_2) & L_2 \cos(\theta_1 + \theta_2) \end{bmatrix} \begin{bmatrix} \dot{\theta}_1 \\ \dot{\theta}_2 \end{bmatrix} \tag{20}$$

Kinetics energy equation:

$$KE = \frac{1}{2} m \dot{x}^2 \tag{21}$$

$$KE_1 = \frac{1}{2} m_1 L_1^2 \dot{\theta}_1^2 \tag{22}$$

$$KE_2 = \frac{1}{2} m_2(L_1^2 \dot{\theta}_1^2) + m_2 L_1 L_2 \cos \theta_2 \left(\dot{\theta}_1^2 + \dot{\theta}_1 \dot{\theta}_2 \right) + \frac{1}{2} m_2 L_2^2 (\dot{\theta}_1^2 + 2\dot{\theta}_1 \dot{\theta}_2 + \dot{\theta}_2^2) \tag{23}$$

Potential Energy equation can be derived below,

$$PE = mgl \tag{24}$$

$$PE_1 = m_1 g L_1 \sin \theta_1 \tag{25}$$

$$PE_2 = m_2 g[L_1 \sin \theta_1 + L_2 \sin(\theta_1 + \theta_2)] \tag{26}$$

Create the Lagrange-Eular Equation using the Lagrangian($\mathcal{L}$) to determine the force acting on the robot.

$$\tau_i = \frac{d}{dt} \left[\frac{\partial \mathcal{L}}{\partial_{\dot{\theta}_i}} \right] - \frac{\partial \mathcal{L}}{\partial \theta_i} \tag{27}$$

$$\begin{aligned} \tau_1 = (m_1 + m_2) L_1^2 \ddot{\theta}_1 &+ 2m_2 L_1 L_2 \cos \theta_2 (\ddot{\theta}_1) - 2m_2 L_1 L_2 \sin \theta_2 (\dot{\theta}_1 \dot{\theta}_2) + m_2 L_1 L_2 \cos \theta_2 (\ddot{\theta}_2) \\ &- m_2 L_1 L_2 \sin \theta_2 (\dot{\theta}_2^2) + m_2 L_2^2 (\ddot{\theta}_1) + m_2 L_2^2 (\ddot{\theta}_2) + (m_1 + m_2) g L_1 \sin \theta_1 \\ &+ m_2 g L_2 \sin(\theta_1 + \theta_2) \end{aligned} \tag{28}$$

$$\tau_2 = m_2 L_1 L_2 \cos \theta_2 \left(\ddot{\theta_1}\right) - m_2 L_1 L_2 \sin \theta_2 \left(\dot{\theta_1}\dot{\theta_2}\right) + m_2 L_2{}^2 \left(\ddot{\theta_1}\right) + m_2 L_2{}^2 \left(\ddot{\theta_2}\right) + m_2\, g\, L_2 \sin(\theta_1 + \theta_2) \tag{29}$$

Substitute into the torque equation below,

$$\tau = D(\theta)\ddot{\theta} + C(\theta,\dot{\theta}) + g(\theta) \tag{30}$$

$$D(\theta) = \begin{bmatrix} (m_1+m_2)L_1{}^2 + 2m_2\, L_1 L_2 \cos \theta_2 + m_2 L_2{}^2 & m_2 L_1 L_2 \cos \theta_2 + m_2 L_2{}^2 \\ m_2\, L_1 L_2 \cos \theta_2 + m_2 L_2{}^2 & m_2 L_2{}^2 \end{bmatrix} \tag{31}$$

$$C(\theta,\dot{\theta}) = \begin{bmatrix} -2m_2 L_1 L_2 \sin \theta_2 \left(\dot{\theta_1}\dot{\theta_2}\right) - m_2 L_1 L_2 \sin \theta_2 \left(\dot{\theta_2}{}^2\right) \\ -m_2 L_1 L_2 \sin \theta_2 \left(\dot{\theta_1}\dot{\theta_2}\right) \end{bmatrix} \tag{32}$$

$$g(\theta) = \begin{bmatrix} (m_1+m_2)\, g\, L_1 \sin \theta_1 + m_2\, g\, L_2 \sin(\theta_1 + \theta_2) \\ m_2\, g\, L_2 \sin(\theta_1 + \theta_2) \end{bmatrix} \tag{33}$$

Mathematical Modelling of the Actuating system
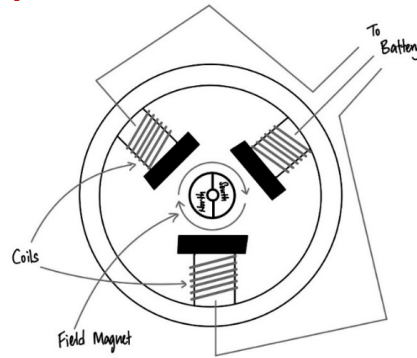
Figure 4. Brushless motor

Consists of a mechanical and an electrical component, is started by the Brushless motor. We can use Newton's law, Kirchhoff's law, and Ohm's law to explain the electrical and mechanical properties of brushless motors [10].

$$[V_{in}(s) - K_b \omega_m] * \frac{1}{(L_a s + R_a)} = I_a(s) \tag{34}$$

$$\omega(s) = K_t * I_a(s) * \frac{1}{(J_m s + b_m)} \tag{35}$$

The transfer function for a brushless motor is calculated by substituting the properties of an electrical component.

$$K_t \frac{1}{(L_a s + R_a)}[V_{in}(s) - K_b \omega_m] = J_m s \omega + b_m \omega \tag{36}$$

The brushless motor is a second order system, according to this equation.

$$G_{speed}(s) = \frac{\omega(s)}{V_{in}(s)} = \frac{K_t}{[(L_a J_m)s^2 + (R_a J_m + b_m L_a)s + (R_a b_m + K_t K_b)]} \tag{37}$$

PID Controller Design

$$F = K_P\, e + K_D\, \dot{e} + K_I \int e\, dt \tag{38}$$

Where $e = q^d - q$, q^d is desired joint angle, K_p, K_i and K_d are proportional, integral and derivative gains of the PID controller, respectively. These equations can be used to express this PID control legislation [11].

$$F = K_P\, e + K_D\, \dot{e} + \xi \tag{39}$$

The control action F is substituted to create the closed-loop equation, gives:

$$D(\ddot{q}) + C(\dot{q}, q) + g(q) = K_P\, e + K_D\, \dot{e} + \xi \tag{40}$$

We can have

$$\ddot{q} = D(q)^{-1}[-C(\dot{q}, q) - g(q)] + F \tag{41}$$

With

$$\hat{F} = D(q)^{-1}F \ \leftrightarrow\ F = D(q)\,\hat{F} \tag{42}$$

So that the system could receive the new (non-physical) input, we detached it.

$$\hat{F} = \begin{bmatrix} f_1 \\ f_2 \end{bmatrix} \tag{43}$$

The physical torque inputs to the system, on the other hand, are

$$\begin{bmatrix} f_{\theta 1} \\ f_{\theta 2} \end{bmatrix} = B(q) \begin{bmatrix} f_1 \\ f_2 \end{bmatrix} \tag{44}$$

The error signal of the system are

$$e(\theta_1) = \theta_{1f} - \theta_1 \tag{45}$$

$$e(\theta_2) = \theta_{2f} - \theta_2 \tag{46}$$

where θ_f is the final positions. The final position is determined by

$$\begin{bmatrix} \theta_{1f} \\ \theta_{2f} \end{bmatrix} = \begin{bmatrix} \dfrac{\pi}{2} \\ -\dfrac{\pi}{2} \end{bmatrix} \tag{47}$$

The starting position is provided by

$$\theta_o = \begin{bmatrix} -\dfrac{\pi}{2} \\ \dfrac{\pi}{2} \end{bmatrix} \tag{48}$$

So, in our case:

$$f_1 = K_{p1}(\theta_{1f} - \theta_1) + K_{D1}\dot{\theta}_1 + K_{I1}\int e(\theta_1)\, dt \tag{49}$$

$$f_2 = K_{p2}(\theta_{2f} - \theta_2) + K_{D2}\dot{\theta}_2 + K_{I2}\int e(\theta_2)\, dt \tag{50}$$

The entire set of control system equations would be

$$\ddot{q} = D(q)^{-1}[-C(\dot{q}, q) - g(q)] + \hat{F} \tag{51}$$

With

$$\hat{F} = \begin{bmatrix} f_1 \\ f_2 \end{bmatrix} = \begin{bmatrix} K_{p1}(\theta_{1f} - \theta_1) + K_{D1}\dot{\theta}_1 + K_{I1}\int e(\theta_1)\, dt \\ K_{p2}(\theta_{2f} - \theta_2) + K_{D2}\dot{\theta}_2 + K_{I2}\int e(\theta_2)\, dt \end{bmatrix} \tag{52}$$

Recalling the physical actual torques

$$\begin{bmatrix} F_{\theta 1} \\ F_{\theta 2} \end{bmatrix} = D(q) \begin{bmatrix} f_1 \\ f_2 \end{bmatrix} \tag{53}$$

Then,

$$\xi_1 = K_{I1}\int e(\theta_1)\, dt \ \leftrightarrow\ \dot{\xi}_1 = K_{I1}\, e_1 \tag{54}$$

$$\xi_2 = K_{I2}\int e(\theta_2)\, dt \ \leftrightarrow\ \dot{\xi}_2 = K_{I2}\, e_2 \tag{55}$$

The system equation is

$$\begin{bmatrix} \ddot{\theta}_1 \\ \ddot{\theta}_2 \end{bmatrix} = D(q)^{-1} [-C(\dot{q},q) - g(q)] + \begin{bmatrix} K_{p1}(\theta_{1f} - \theta_1) + K_{D1}\dot{\theta}_1 + \dot{\xi}_1 \\ K_{p2}(\theta_{2f} - \theta_2) + K_{D2}\dot{\theta}_2 + \dot{\xi}_2 \end{bmatrix} \tag{56}$$

EXPERIMENTAL RESULTS
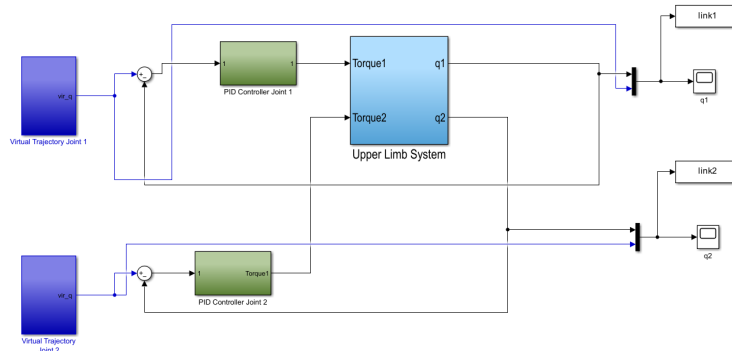
Figure 5. Simulink Design
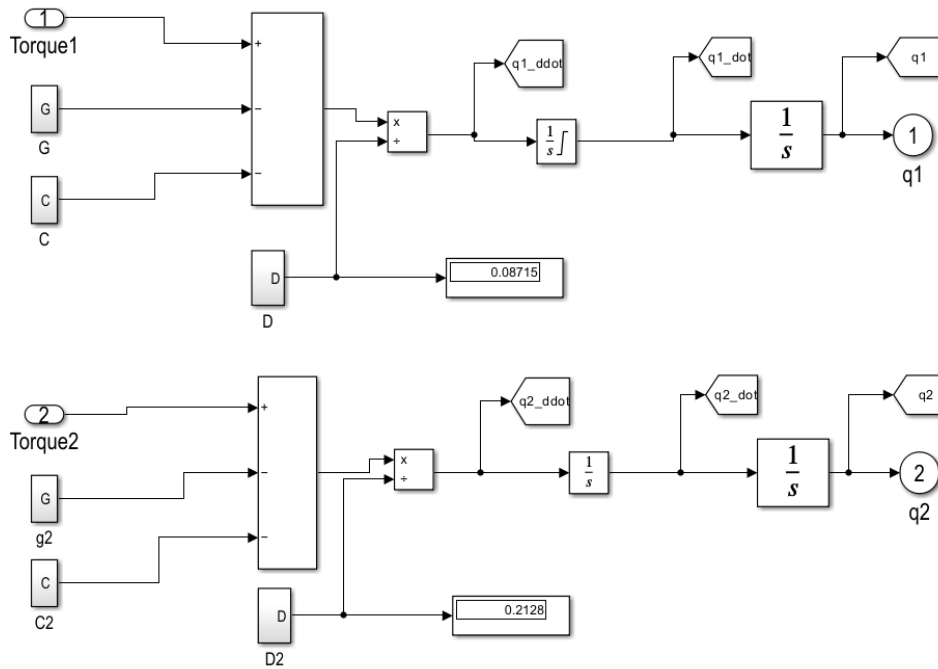
Figure 6. Upper Limb System

Table 2. This is the combination graph of desired, without controller, PI, PD and PID in Simulation
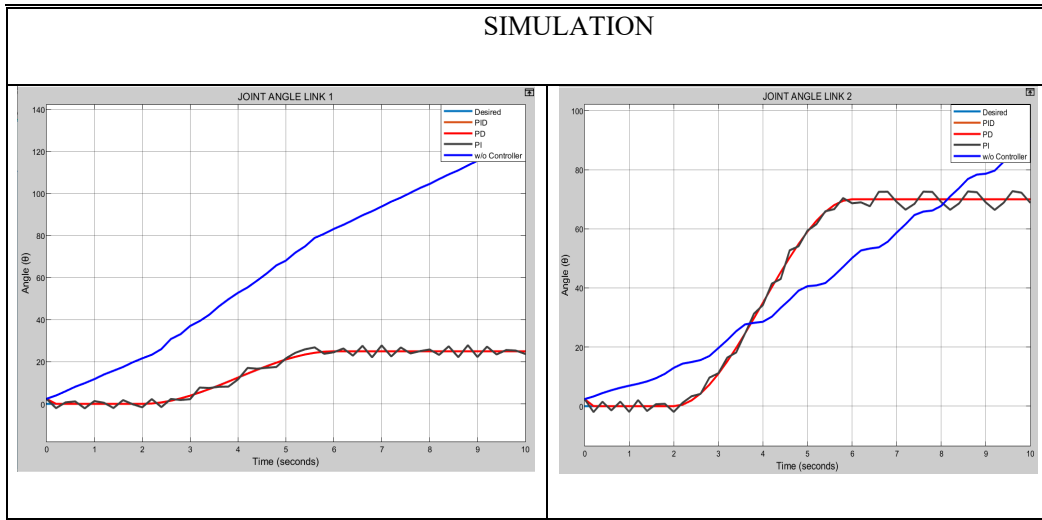
Table 3. This error and RMSE table is based on links 1 and 2

Error		
	Simulation (ε)(%)	
Link	Link 1	Link 2
Without Controller	22.44	29.53
PI	1.37	0.86
PD	0.0056	0.0044
PID	0.0024	0.0026
RMSE		
	Simulation (ε)(%)	
Link	Link 1	Link 2
Without Controller	28.88	25.4124
PI	1.4434	0.7732
PD	0.0195	0.0421
PID	0.0093	0.0100

Through the error and RMSE table, we can see that the PID Controller's error value and the RMSE value is the least.

The response without a controller demonstrates the limitations of the motor's inherent dynamics. The inability to achieve the desired behaviour indicates the need for a control mechanism to regulate the motor's speed or position accurately. Without a controller, the system may experience significant errors, sluggish response times, and instability, making it unsuitable for precise rehabilitation movements.

With a PI controller, the system's response shows improvement compared to the case without a controller. The integral action of the PI controller allows for the gradual elimination of steady state errors, enabling the system to track the desired response more accurately. However, the observed damping suggests a trade off between achieving accurate tracking and the speed of response. It may be necessary to fine tune the PI controller's gains to strike a balance between accuracy and responsiveness.

The response with a PD controller exhibits similar behaviour to the PID controller, showcasing the benefits of incorporating derivative action. The derivative term allows for quicker response times by considering the rate of change of the error signal. Consequently, the PD controller offers improved damping, reducing overshoot and oscillations in the system's response. It provides more precise tracking of the desired response compared to the PI controller.

The response with a PID controller integrates the proportional, integral, and derivative actions to provide a comprehensive control solution. It achieves accurate tracking of the desired response, faster response times, reduced steady state errors, and improved damping. By balancing the three control actions, the PID controller can effectively regulate the motor's speed or position in the rehab robot. Fine tuning the gains of the PID controller can further enhance its performance and ensure the desired response is achieved optimally.

In summary, the comparison highlights the necessity of a controller for precise control of the motor in a rehab robot. While the response without a controller exhibits limitations, the addition of a control mechanism significantly improves the system's performance. The PI controller reduces steady state errors but may exhibit damping, while the PD and PID controllers offer enhanced damping and faster response times. The PID controller, leveraging all three control actions, provides the most comprehensive solution by achieving accurate tracking, reducing errors, and ensuring stability.

It is crucial to consider the specific requirements of the rehab robot, such as the desired response characteristics, sensitivity to disturbances, and trade offs between accuracy and responsiveness. Through iterative simulations and fine tuning of the controller parameters, the most suitable control method and its associated gains can be determined to achieve the desired response effectively and facilitate successful rehabilitation movements.

CONCLUSION

In conclusion, PID controller plays a crucial role in achieving precise and accurate arm movements. It can be concluded that a variety of factors, including system dynamics, tuning parameters, setpoints, simulation time, sample rate, and sensitivity to noise or disturbances, can be attributed to the observation that the PID and PD controllers produce similar results while the PI controller displays damping behavior in the simulation of position control for two DC motor with an encoder. A greater understanding of the behaviours of the controllers will result from looking into and addressing these factors, which will also make it easier to optimize them for the application in question.

As a result, the main objective of developing a controller for the rehab robot and subsequent objective have been successfully achieved. PID Controller exhibits the best performance. Choosing a PID controller is therefore the best option.

REFERENCES

[1]   "Learn about stroke | World Stroke Organization." https://www.world-stroke.org/world-stroke-day-campaign/why-stroke-matters/learn-about-stroke (accessed Jun. 24, 2023).

[2]   A. Mohebbi, "Human-Robot Interaction in Rehabilitation and Assistance: a Review," *Current Robotics Reports 2020 1:3*, vol. 1, no. 3, pp. 131–144, Aug. 2020, doi: 10.1007/S43154-020-00015-4.

[3]   B. French *et al.*, "Repetitive task training for improving functional ability after stroke," *Cochrane Database Syst Rev*, vol. 2016, no. 11, Nov. 2016, doi: 10.1002/14651858.CD006073.PUB3.

[4]   H. M. Qassim and W. Z. Wan Hasan, "A review on upper limb rehabilitation robots," *Applied Sciences (Switzerland)*, vol. 10, no. 19. MDPI AG, pp. 1–18, Oct. 01, 2020. doi: 10.3390/app10196976.

[5]   M. Mahmud, S. M. A. Motakabber, A. H. M. Zahirul Alam, and A. N. Nordin, "Adaptive PID Controller Using for Speed Control of the BLDC Motor," *IEEE International Conference on Semiconductor Electronics, Proceedings, ICSE*, vol. 2020-July, pp. 168–171, Jul. 2020, doi: 10.1109/ICSE49846.2020.9166883.

[6]   A. Okubanjo, O. Oluwadamilola, O. Martins, and O. Olaluwoye, "Modeling of 2-DOF Robot Arm and Control," *Futo Journal Series (FUTOJNLS)*, vol. 3, no. 2, pp. 80–92, 2017, [Online]. Available: www.futojnls.org

[7]   T. P. Singh, P. Suresh, and S. Chandan, "Forward and Inverse Kinematic Analysis of Robotic Manipulators," *International Research Journal of Engineering and Technology*, 2017, [Online]. Available: www.irjet.net

[8]   K. Zheng, T. Shen, and Y. Yao, "Input constrained positioning control for a class of Eular-Lagrange systems with discontinuities," *Proceedings of the IEEE Conference on Decision and Control*, pp. 4007–4012, 2007, doi: 10.1109/CDC.2007.4434581.

[9]   H. Harry Asada, "Introduction to Chapter 7 Dynamics."

[10]   "Mathematical modeling and Simulation of Brushless DC motor with Ideal Back EMF for a Precision speed control."

[11]   O. Bethoux, "PID controller design," in *Encyclopedia of Electrical and Electronic Power Engineering*, Elsevier, 2023, pp. 261–267. doi: 10.1016/b978-0-12-821204-2.00102-1.